First purely inorganic polyoxotungstates constructed from dimeric tungstoantimonate-based iron–rare-earth heterometallic fragments

Lijuan Chen, Jing Cao, Xinghua Li, Xing Ma, Jie Luo,* and Junwei Zhao*

Henan Key Laboratory of Polyoxometalate Chemistry, Institute of Molecular and Crystal Engineering, College of Chemistry and Chemical Engineering, Henan University, Kaifeng, Henan 475004, P. R. China. Email: luojie@henu.edu.cn, zhaojunwei@henu.edu.cn

Electronic Supplementary Information

Table S1 Summary on the examples involving isomerization of $[B\text{-}\alpha\text{-}SbW_9O_{33}]^{9-} \rightarrow [B\text{-}\beta\text{-}SbW_9O_{33}]^{9-}$

Public date	pH	Synthetic method	Reaction system
2002	3.0	Conventional solution	$[Fe_4(H_2O)_{10}(\beta\text{-}SbW_9O_{33})_2]$[6–13]
2008	2.0	Conventional solution	$[Fe_4(H_2O)_8(\beta\text{-}SbW_9O_{33})_2]$[6–32a]
2008	3.0	Conventional solution	$[Fe_4(C_2O_4)_4(H_2O)_2(\beta\text{-}SbW_9O_{33})_2]$[14–32a]
2008	4.5	Conventional solution	$[Fe_4(C_2O_4)_4(\beta\text{-}SbW_9O_{33})_2]$[14–32a]
2009	6.0	Conventional solution	$[Sb_2W_{20}O_{70}(RuC_6H_6)_2]_3$[10–8]
2009	6.0	Conventional solution	$[Sb_2W_{20}O_{70}(RuC_{10}H_{14})_2]_3$[10–8]
2010	3.0	Conventional solution	$[\{Sn(CH_3)_2\}_3(H_2O)_4(\beta\text{-}SbW_9O_{33})]$[3–32b]
2011	5.53	Conventional solution	$[\{Co(H_2O)_3\}_2Co(H_2O)_2W(H_2O)_2(B\text{-}\beta\text{-}SbW_9O_{33})_2]$[6–32c]
2011	5.50	Conventional solution	$[Mn_{3.5}(H_2O)_7W_{0.5}(H_2O)(B\text{-}\beta\text{-}SbW_9O_{33})_2]$[8–32c]
2011	3.0	Conventional solution	$[\{Y(H_2O)_7\}_4Sb_2W_{22}O_{76}]$[2–31]
2012	1.5	Conventional solution	$[\{Ru^{IV}_4O_6(H_2O)_9\}_2Sb_2W_{20}O_{68}(OH)_2]$[4–10]
2013	3.0	Conventional solution	$[Al^{III}_4(H_2O)_{10}(\beta\text{-}SbW_9O_{33}H)_2]$[4–14]
2013	6.0	Conventional solution	$[Sb_2W_{20}O_{70}\{Mn(CO)_3\}_2]$[12–11]
2013	3.0	Conventional solution	$[Ln(H_2O)_4Sb_2W_{21}O_{72}(OH)]$[10– 22]
2013	4.8	Conventional solution	$[Ln_2(H_2O)_8Sb_2W_{20}O_{70})]$[8–22]

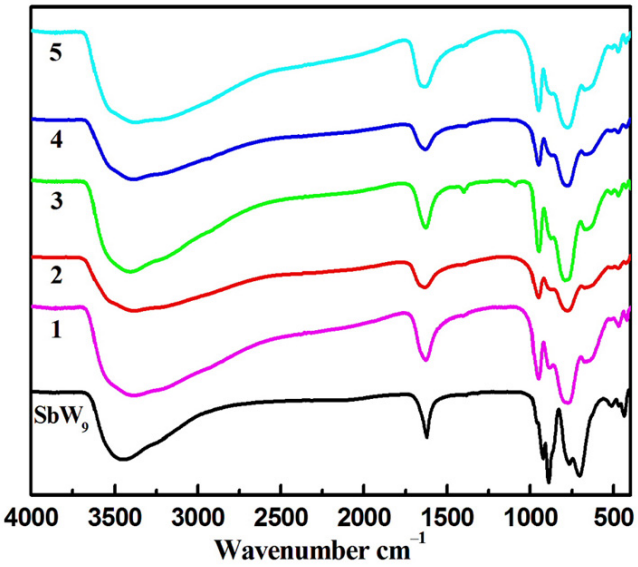

Fig. S1. IR spectra of **1–5** and $Na_9[B\text{-}\alpha\text{-}SbW_9O_{33}]\cdot 19.5H_2O$ (SbW_9)

The discussion on electrochemical properties of 1 and 2:

Additionally, the influences of the scan rate on the electrochemical behaviors of **1** and **2** have been measured in the potential range of 0.9 to −0.8 V in various scan rates in the aforementioned conditions (Fig. S2, S3b). It elucidates the variety of the cathodic and anodic peak currents of the W^{VI}-based wave with different scan rates, which unambiguously indicate that with increasing of the scan rate from 15 to 40 $mV\cdot s^{-1}$ for **1** and 30 to 100 $mV\cdot s^{-1}$ for **2**, the intensity of the

first W-based redox pair (I-I') gradually increases while the second W^{VI}-based redox couple (II-II') shows a weaken rising trend. It can be seen that with increasing of the scan rate, the cathodic peak potential gradually shifts to the negative direction whereas the corresponding anodic peak potential gradually move to the positive direction, as a consequence, the peak-to-peak separation between the according cathodic and anodic waves enlarges, but the locations of their mean waves are not significantly affected, that is to say that these peak positions almost no shifts in principle as described in the previous reported for other POMs.[1] Fig. S4 exhibits the variation of the peak current intensity of the W-based reduction wave (I') with the scan rate [for **1** the scan rate changing from 15 to 40 $mV \cdot s^{-1}$ and for **2** the scan rate changing between 30 and 100 $mV \cdot s^{-1}$]. The peak current intensity is proportional to the square root of the scan rate, enucleating a characteristic diffusion-controlled electron-transfer process under these scan rate conditions.[2] It is well-known that the reduction of POMs results in an accumulation of negative charge, which increases the basicity of the POA and the reduction process may be accompanied by concomitant protonation.[3] The influence of the variation of the pH of the supporting electrolyte on the electrochemical behavior of **1** and **2** have also been probed (Fig. S5, S6). It can be clearly seen that with increasing the pH, their entire cyclic voltammograms move toward the negative potential direction and peak currents gradually decrease (Tables S2, S3), which hints the important role of protons in the electrochemistry of POMs. This observation coincides with the previous reports.[4]

1 (*a*) Z. G. Han, Y. L. Zhao, J. Peng, Q. Liu and E. B. Wang, *Electrochim. Acta*, 2005, **51**, 218; (*b*) B. Keita, P. Mialane, F. Sécheresse, P. de Oliveira and L. Nadjo, *Electrochem. Commun.*, 2007, **9**, 164.

2 (*a*) X. L. Wang, Z. H. Kang, E. B. Wang and C. W. Hu, *Materials Letters*, 2002, **56**, 393; (*b*) M. Ibrahim, A. Haider, Y. h. Lan, B. S. Bassil, A. M. Carey, R. J. Liu, G. J. Zhang, B. Keita, W. H. Li, G. E. Kostakis, A. K. Powell and U. Kortz, *Inorg. Chem.*, 2014, **53**, 5179.

3 (*a*) M. Ammam and E. B. Easton, *Electrochim. Acta,* 2011, **56**, 2847; (*b*) B. Keita, K. Essaadi and L. Nadjo, *J. Electroanal. Chem. Interfacial Electrochem.*. 1989, **259**, 127.

4 (*a*) B. Keita, Y. W. Lu, L. Nadjo and R. Contant, *Electrochem. Commun.*, 2000, **2**, 720; (*b*) M. Ibrahim, Y. X. Xiang, B. S. Bassil, Y. H. Lan, A. K. Powell, P. de Oliveira, B. Keita and U. Kortz, *Inorg. Chem.* 2013, **52**, 8399; (*c*) W. C. Chen, X. L. Wang, Y. Q. Jiao, P. Huang, E. L. Zhou, Z. M. Su and K. Z. Shao, *Inorg. Chem.*, 2014, **53**, 9486.

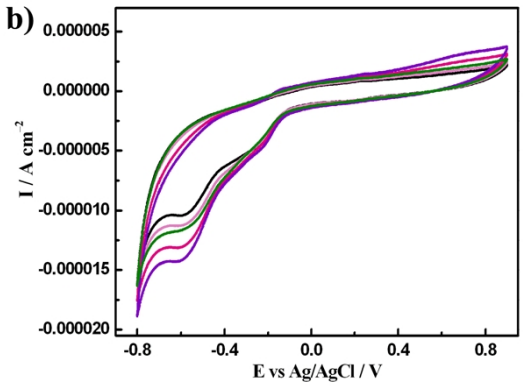

Fig. S2 Cyclic voltammograms at different scan rates: from inside to outside: 15, 20, 25, 30 and 40 mV·s^{-1}.

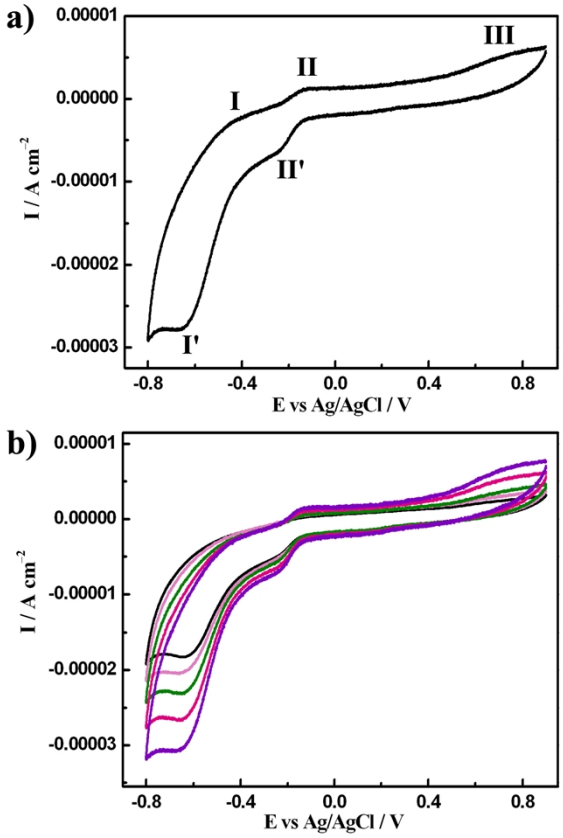

Fig. S3 (a) Cyclic voltammogram of **2** (concentration: 1.73 × 10^{-4} mol·L^{-1}) in 0.5 mol·L^{-1} Na_2SO_4 + H_2SO_4 aqueous solution (pH = 1.58). Scan rate: 80 mV·s^{-1}. (b) Cyclic voltammograms at different scan rates: from inside to outside: 30, 40, 50, 70 and 100 mV·s^{-1}.

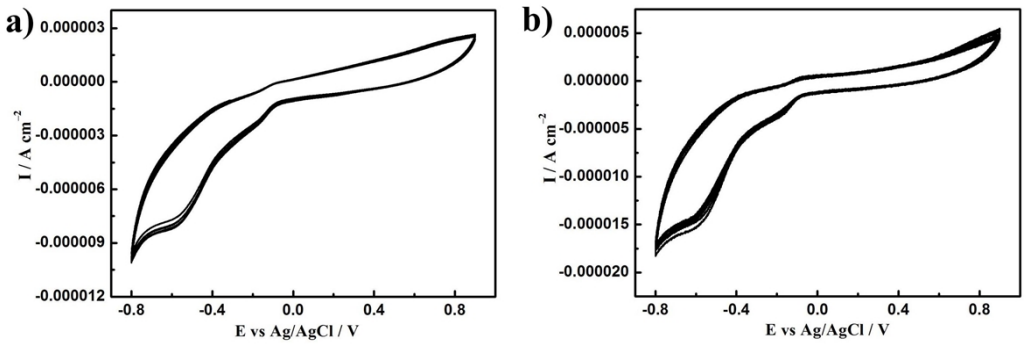

Fig. S4 (a) Cyclic voltammograms of **1** (concentration: 1.73×10^{-4} mol·L^{-1}) in 0.5 mol·L^{-1} $Na_2SO_4 + H_2SO_4$ aqueous solution (pH = 1.44) for 10 cycles. Scan rate: 30 mV·s^{-1}. (b) Cyclic voltammograms of **2** (concentration: 1.47×10^{-4} mol·L^{-1}) in 0.5 mol·L^{-1} $Na_2SO_4 + H_2SO_4$ aqueous solution (pH = 1.58) for 10 cycles. Scan rate: 80 mV·s^{-1}.

Table S2 The peak potentials for all the redox waves for 1 determined by CV in 0.5 mol·L^{-1} $H_2SO_4 + Na_2SO_4$ aqueous solution at pH = 0.85, 1.44 and 2.20. Scan rate: 30 mV·s^{-1}.

pH	E_{pa} (V)	E_{pc} (V)	$E_{1/2}$ (V)	ΔE_p (mV)
0.85	−0.393	−0.544	−0.469	151
	−0.090	−0.183	−0.137	93
	0.769			
1.44	−0.486	−0.646	−0.566	178
	−0.147	−0.247	−0.197	100
	0.749			
2.20	−0.568	−0.703	−0.636	135
	−0.168	−0.308	−0.238	140
	0.740			

Table S3 The peak potentials for all the redox waves determined by CV in 0.5 mol·L^{-1} $H_2SO_4 + Na_2SO_4$ solution at pH = 0.91, 1.58 and 2.69 for 2. Scan rate: 80 mV·s^{-1}

pH	E_{pa} (V)	E_{pc} (V)	$E_{1/2}$ (V)	ΔE_p (mV)
0.91	−0.362	−0.586	−0.474	224
	−0.109	−0.187	−0.148	78
	0.781			
1.58	−0.438	−0.661	−0.550	223
	−0.131	−0.238	−0.185	107
	0.734			
2.69	−0.543	−0.755	−0.649	212
	−0.194	−0.379	−0.287	185
	0.728			

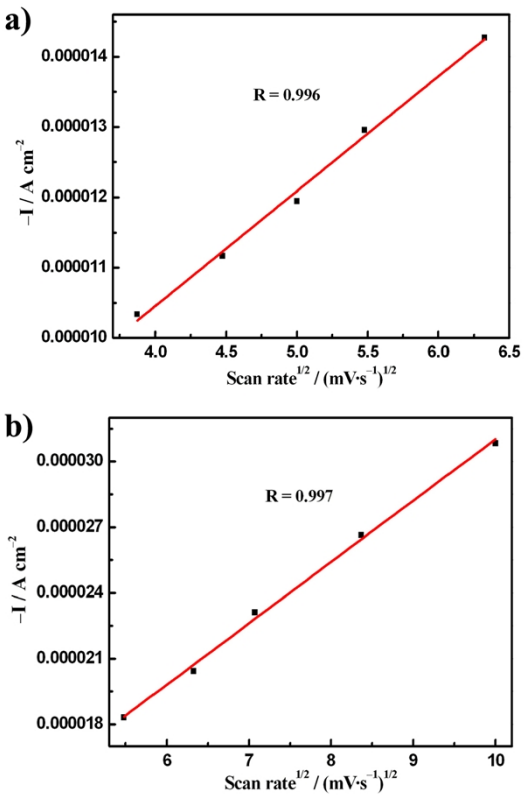

Fig. S5 The variation of the cathodic peak current (I') intensity as a function of the square root of the scan rate for **1** (a) and **2** (b).

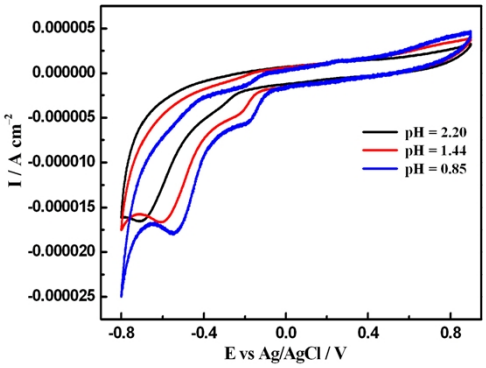

Fig. S6 (a) Variation of cyclic voltammograms of **1** (concentration: 1.73 × 10^{-4} mol·L^{-1}) at different pH values: pH = 2.20 (black), 1.44 (red), 0.85 (blue) in 0.5 mol·L^{-1} Na_2SO_4 + H_2SO_4 aqueous solution. Scan rate: 30 mV·s^{-1}.

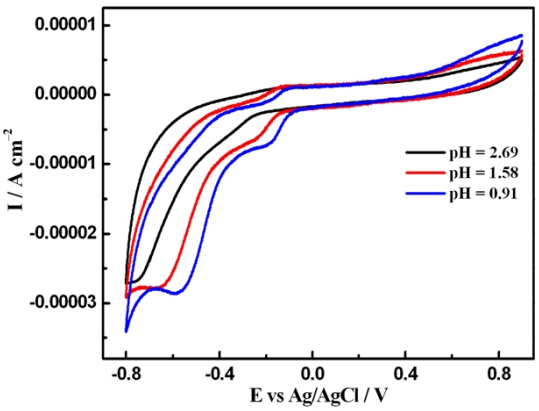

Fig. S7 (a) Cyclic voltammograms of **2** (concentration: 1.47×10^{-4} mol·L^{-1}) at different pH values: pH = 2.69 (black), 1.58 (red), 0.91 (blue) in 0.5 mol·L^{-1} $Na_2SO_4 + H_2SO_4$ aqueous solution. Scan rate: 80 mV·s^{-1}.

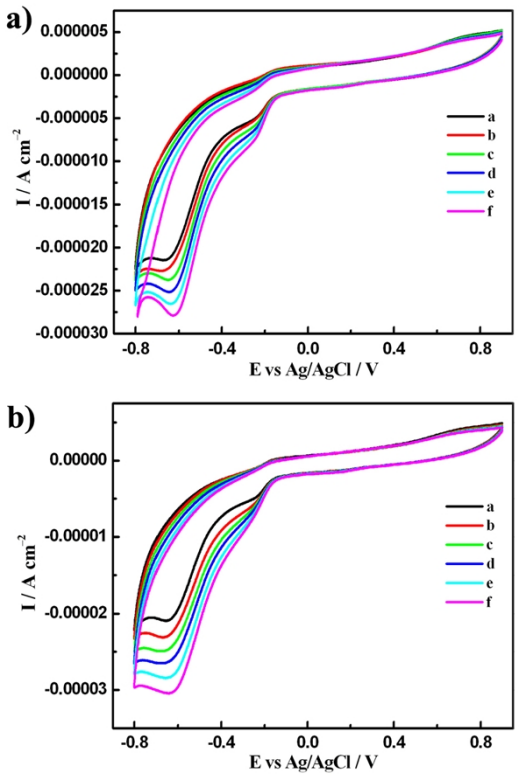

Fig. S8 (a) Cyclic voltammograms of **2** (concentrations: 1.47×10^{-4} mol·L^{-1}) in pH = 1.58 0.5 mol·L^{-1} $Na_2SO_4 + H_2SO_4$ aqueous solution with addition of various concentrations of $NaNO_2$ (a: 0, b: 1×10^{-5}, c: 3×10^{-5}, d: 5×10^{-5}, e: 9×10^{-5}, f: 1.5×10^{-4} mol·L^{-1}). (b) Cyclic voltammograms of **2** (concentrations: 1.47×10^{-4} mol·L^{-1}) in pH = 1.58 0.5 mol·L^{-1} $Na_2SO_4 + H_2SO_4$ aqueous solution with addition of various concentrations of $NaBrO_3$ (a: 0, b: 1×10^{-5}, c: 2×10^{-5}, d: 3×10^{-5}, e: 4×10^{-5}, f: 5×10^{-5} mol·L^{-1}). Scan rate: 80 mV·s^{-1}.

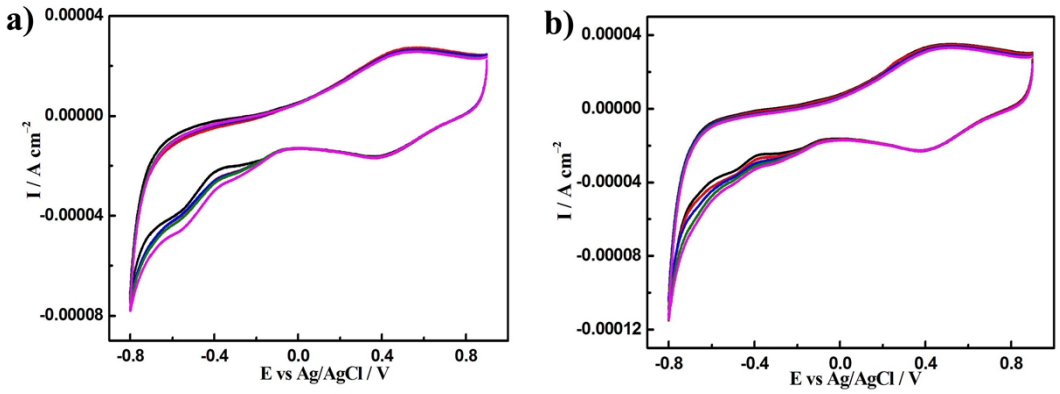

Fig. S9 (a) Cyclic voltammograms of $Na_9[B\text{-}\alpha\text{-}SbW_9O_{33}]\cdot 19.5H_2O$ (concentration: 3.46×10^{-4} mol·L^{-1}) in pH = 1.50 0.5 mol·L^{-1} $Na_2SO_4 + H_2SO_4$ aqueous solution with addition of various concentrations of $NaNO_2$ (a: 0, b: 3×10^{-5}, c: 7×10^{-5}, d: 1.1×10^{-4}, e: 1.5×10^{-4} mol·L^{-1}). Scan rate: 30 mV·s^{-1}. (b) Cyclic voltammograms of $Na_9[B\text{-}\alpha\text{-}SbW_9O_{33}]\cdot 19.5H_2O$ (concentration: 3.46×10^{-4} mol·L^{-1}) in pH = 1.50 0.5 mol·L^{-1} $Na_2SO_4 + H_2SO_4$ aqueous solution with addition of various concentrations of $NaBrO_3$ (a: 0, b: 1×10^{-5}, c: 4×10^{-5}, d: 7×10^{-5}, e: 9×10^{-5}). Scan rate: 30 mV·s^{-1}.

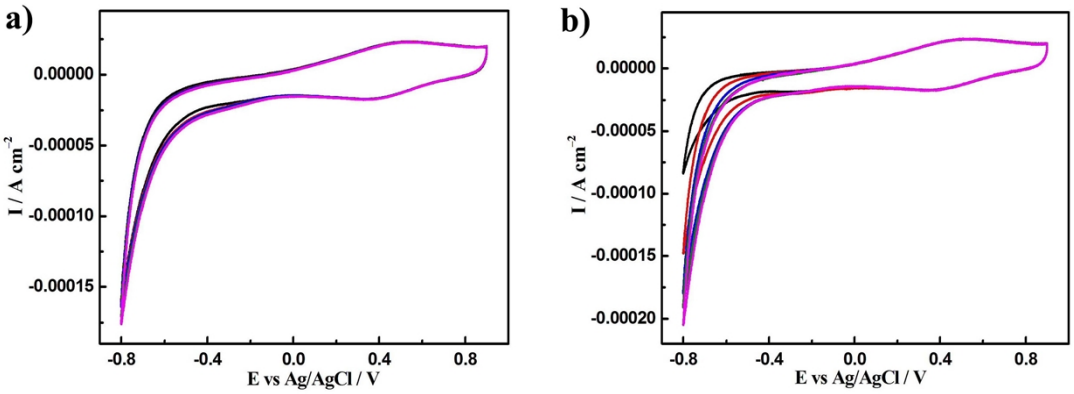

Fig. S10 (a) Cyclic voltammograms of $FeCl_3\cdot 6H_2O$ (concentration: 6.92×10^{-4} mol·L^{-1}) in pH = 1.50 0.5 mol·L^{-1} $Na_2SO_4 + H_2SO_4$ aqueous solution with addition of various concentrations of $NaNO_2$ (a: 0, b: 3×10^{-5}, c: 7×10^{-5}, d: 1.1×10^{-4}, e: 1.5×10^{-4} mol·L^{-1}). Scan rate: 30 mV·s^{-1}. (b) Cyclic voltammograms of $FeCl_3\cdot 6H_2O$ (concentration: 3.46×10^{-4} mol·L^{-1}) in pH = 1.50 0.5 mol·L^{-1} $Na_2SO_4 + H_2SO_4$ aqueous solution with addition of various concentrations of $NaBrO_3$ (a: 0, b: 1×10^{-5}, c: 3×10^{-5}, d: 7×10^{-5}, e: 1.3×10^{-4}). Scan rate: 30 mV·s^{-1}.

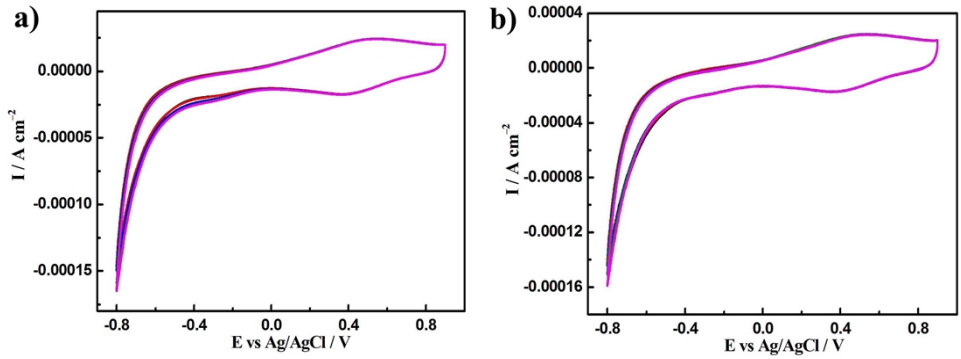

Fig. S11 (a) Cyclic voltammograms of $PrCl_3 \cdot 6H_2O$ (concentration: 3.46×10^{-4} mol·L^{-1}) in pH = 1.50 0.5 mol·L^{-1} $Na_2SO_4 + H_2SO_4$ aqueous solution with addition of various concentrations of $NaNO_2$ (a: 0, b: 1×10^{-5}, c: 7×10^{-5}, d: 1.1×10^{-4}, e: 1.5×10^{-4} mol·L^{-1}). Scan rate: 30 mV·s^{-1}. (b) Cyclic voltammograms of $PrCl_3 \cdot 6H_2O$ (concentration: 3.46×10^{-4} mol·L^{-1}) in pH = 1.50 0.5 mol·L^{-1} $Na_2SO_4 + H_2SO_4$ aqueous solution with addition of various concentrations of $NaBrO_3$ (a: 0, b: 1×10^{-5}, c: 5×10^{-5}, d: 9×10^{-5}, e: 1.3×10^{-4}). Scan rate: 30 mV·s^{-1}.

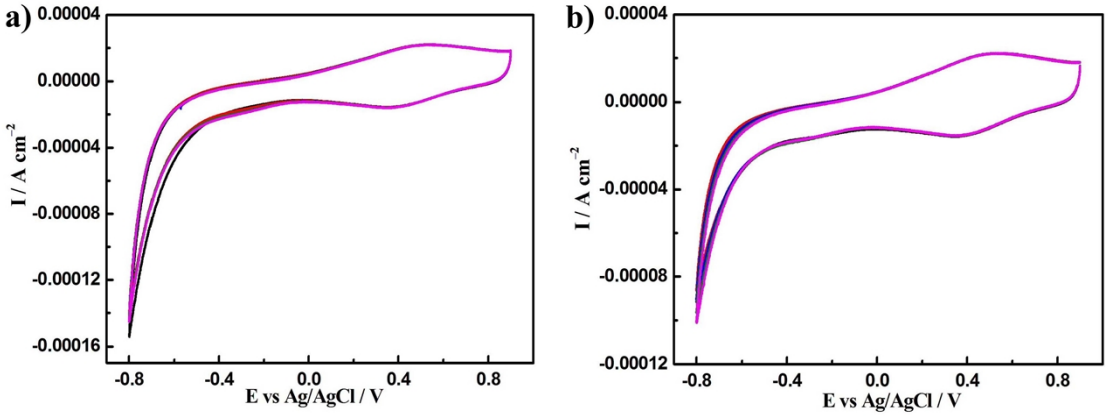

Fig. S12 (a) Cyclic voltammograms of $TbCl_3 \cdot 6H_2O$ (concentration: 3.46×10^{-4} mol·L^{-1}) in pH = 1.50 0.5 mol·L^{-1} $Na_2SO_4 + H_2SO_4$ aqueous solution with addition of various concentrations of $NaNO_2$ (a: 0, b: 1×10^{-5}, c: 7×10^{-5}, d: 1.1×10^{-4}, e: 1.7×10^{-4} mol·L^{-1}). San rate: 30 mV·s^{-1}. (b) Cyclic voltammograms of $TbCl_3 \cdot 6H_2O$ (concentration: 3.46×10^{-4} mol·L^{-1}) in pH = 1.50 0.5 mol·L^{-1} $Na_2SO_4 + H_2SO_4$ aqueous solution with addition of various concentrations of $NaBrO_3$ (a: 0, b: 1×10^{-5}, c: 7×10^{-5}, d: 1.1×10^{-4}, e: 1.7×10^{-4}). Scan rate: 30 mV·s^{-1}.

Table S4 The CAT values of 1 and 2 for the nitrite reduction.

Substrate ($NaNO_2$/ mol·L^{-1})	CAT for **1** (%)	CAT for **2** (%)
1×10^{-5}	4.78	4.55
3×10^{-5}	12.07	9.89
1.5×10^{-4}	38.08	29.31

Table S5 The CAT values of **1** and **2** for the bromate reduction.

Substrate ($NaBrO_3$/ mol·L^{-1})	CAT for **1** (%)	CAT for **2** (%)
1×10^{-5}	10.65	10.54
3×10^{-5}	29.54	26.31
5×10^{-5}	51.04	45.38